Stable isotopes of water vapor in the vadose zone: A review of measurement and modeling techniques

Keir Soderberg[1], Stephen P. Good[1], Lixin Wang[2] and Kelly Caylor[1]

1 – Department of Civil and Environmental Engineering, Princeton University

2 – School of Civil and Environmental Engineering, University of New South Wales

Abstract

The stable isotopes of soil water vapor are useful tracers of hydrologic processes occurring in the vadose zone. The measurement of soil water vapor isotopic composition ($\delta^{18}O$, $\delta^{2}H$) is challenging due to difficulties inherent in sampling vadose zone airspace *in situ*. Historically, these parameters have therefore been modeled as opposed to directly measured, and typically soil water vapor is treated as being in isotopic equilibrium with liquid soil water. We present a review of the measurement and modeling of soil water vapor isotopes, with implications for studies of the soil-plant-atmosphere continuum. We also present a case study with *in situ* measurements from a soil profile in a semi-arid African savanna, which supports the assumption of liquid-vapor isotopic equilibrium. A contribution of this work is to introduce the effect of soil water potential (ψ) on kinetic fractionation during soil evaporation within the Craig-Gordon modeling framework. Including ψ in these calculations becomes important for relatively dry soils (ψ < -10 MPa). Additionally, we assert that the recent development of laser-based isotope analytical systems may allow for the regular *in situ* measurement of the vadose zone isotopic composition of water in the vapor phase. Wet soils pose particular sampling difficulties, and we discuss novel techniques being developed to address these issues.

This is the author's manuscript of the article published in final edited form as:
Soderberg, K., Good, S. P., Wang, L., & Caylor, K. (2012). Stable isotopes of water vapor in the vadose zone: A review of measurement and modeling techniques. Vadose Zone Journal, 11(3). http://dx.doi.org/10.2136/vzj2011.0165

Definitions

The isotope nomenclature used here is consistent with the most recent guidelines (Coplen, 2011) where the decimal values are used in all calculations and "per mil" (‰) values are for display purposes only. We use the term "vapor" to refer to water vapor only, and other gaseous constituents are referred to as "gas". We are explicit about the direction of the isotopic fractionation factors (e.g. $\alpha_{L/V} = R_L/R_V = \varepsilon_{L/V} + 1$), and where no isotope is specified, α can refer to either oxygen or hydrogen fractionation.

a_w	thermodynamic activity of water [-]
D	diffusion coefficient [$m^2\ s^{-1}$], with subscript i indicating the minor isotopologue
$\delta_A, \delta_E, \delta_L, \delta_V$	relative difference of isotope ratios (e.g. $\delta^{18}O = ({}^{18}R/{}^{18}R_{VSMOW} - 1)$) of the atmosphere, evaporate, soil liquid, and soil vapor, respectively [-]
α_e, α_k	equilibrium and kinetic isotopic fractionation factor (e.g. $\alpha_{e,L/V} = R_L/R_V$) [-]
ε_k	kinetic isotopic fractionation ($\varepsilon_k = \alpha_k - 1$) [-]
e_{s0}, e_{sA}	saturation vapor pressure at the evaporating surface and in the atmosphere, respectively [kPa]
θ_0, θ_s, θ_r	volumetric water content of the evaporating surface, saturated and residual water contents, respectively [$m^3\ m^{-3}$]
ρ_w	density of water [$kg\ m^{-3}$]
‰	per mil [-]
ψ_0	water potential at the evaporating surface [MPa]
n	aerodynamic parameter for adjusting diffusivity ratios [-]

h_A, h_0 humidity of the atmosphere and evaporating surface; h_A' is normalized to the evaporating surface [-]

${}^{i}R_p$ isotope ratio of minor isotopologue i to the abundant isotopologue in phase p

R ideal gas constant [L kPa mol^{-1} K^{-1}], distinguished from the isotope ratio (e.g. ${}^{18}R_L$) by having no superscripts or subscripts

T_A, T_0 temperature of the atmosphere and evaporating surface [K]

1. Introduction

Soil water dynamics are the part of the hydrologic cycle that is most directly relevant to vegetation dynamics and productivity (e.g., Rodriguez-Iturbe and Porporato, 2004). Measuring the presence, character and fate of soil water has become standard in agricultural and ecosystem science. The stable isotopes of liquid soil water are routinely measured to investigate processes related to plant water uptake such as relative rooting depth (Jackson et al., 1999), recharge rates (Cane and Clark, 1999), and hydraulic redistribution (Dawson, 1993). The isotope values of liquid soil water change in response to fractionation processes such as evaporation and condensation (Gat, 1996), and are thus dynamically linked to the isotope values of the soil water vapor. The isotopic composition of the vapor component of soil water has been much less studied than the liquid water component, mainly due to sampling difficulties. However, the recent development of laser-based isotope analysis may allow for rapid, *in situ* measurement of soil vapor isotopes. Here we review the measurement and modeling of soil water vapor isotopes, with a focus on the implications of isotope fractionation processes on our understanding of ecohydrology.

The stable isotopic composition of water (δ) is defined as $\delta = ({}^{i}R/{}^{i}R_{std} - 1)$, where ${}^{i}R$ is the ratio of a rare (denoted i, e.g., ^{18}O) to common isotope ($^{2}H/^{1}H$ or $^{18}O/^{16}O$) in sample water, and ${}^{i}R_{std}$ is the same ratio of the international standard, *VSMOW* (De Laeter et al., 2003; Gonfiantini, 1978). The stable isotope composition of water is a powerful process tracer in ecology, plant physiology, meteorology and hydrology (e.g., Brunel et al., 1992; Dawson et al., 2002; Gat, 1996; Wang et al., 2010). One of the three landmark papers that were identified in physical meteorology (Lee and Massman, 2011) is about stable isotopes of water. In this paper, Craig (1961) reported the discovery of a robust relationship between oxygen and hydrogen isotopic

abundance in precipitation, a relationship now widely known as the Global Meteoric Water Line (GMWL), which has become part of general scientific language today.

The stable isotopic composition of soil water has been used to trace water movement in the unsaturated zone (Barnes and Allison, 1988), estimate evaporation rate (Allison and Barnes, 1983) and trace groundwater recharge (Cane and Clark, 1999). The isotopic composition of water in stems and roots usually reflects the isotopic composition of plant-available soil water (Flanagan and Ehleringer, 1991; White et al., 1985), although exceptions can exist in extreme environments (Ellsworth and Williams, 2007). Thus, the isotopic composition of plant stem water has been widely used to identify plant water sources (e.g., irrigation, rainwater, groundwater) in various ecosystems (Dawson, 1996; Ehleringer and Dawson, 1992; Ehleringer et al., 1999). At the watershed scale, water isotopes can be used to trace the catchment water movement and storage mechanisms (Brooks et al., 2010). At the global scale, water isotopes can be used to explore global scale land-atmosphere interaction (Hoffmann et al., 2000), to reconstruct the past environmental parameters such as ambient temperature and relative humidity (e.g., Helliker and Richter, 2008) and to constrain primary productivity (Welp et al., 2011).

Evaporation from soil, and thus the underlying soil water vapor, can play an important role in the hydrologic cycle, particularly in dryland ecosystems (D'Odorico et al., 2007; Nicholson, 2000; Risi et al., 2010a; Yoshimura et al., 2006). These ecosystems, such as semi-arid African savannas, often have significant unvegetated patches and large diurnal and seasonal shifts in temperature and water availability leading to important feedbacks in vegetation structure (D'Odorico et al., 2007; Nicholson, 2000; Scanlon et al., 2007). For soils in wetter environments, water movement in the liquid phase is more prominent than in the vapor phase, although vapor flux out of the soil could still be a significant component of the water cycle in these

environments. These wet soils pose particular vapor sampling difficulties, which are discussed in Section 2.2.

The redistribution of soil water from wetter layers to drier layers at night ("hydraulic redistribution") is a widespread phenomenon affecting plant community dynamics and the evaporative flux of soil water (e.g., Feddes et al., 2001; Mooney et al., 1980). However, in dry soils, diurnal shifts in soil temperature gradients can induce the movement of soil water vapor, which flows from warmer to cooler layers where it may condense (Abramova, 1969; Bittelli et al., 2008; Harmathy, 1969; Philip and de Vries, 1957) and become available to plants (Abramova, 1969). This vapor movement can occur in bare soil and have the same effect as hydraulic redistribution. For example, observations of soil water content demonstrated that the movement of water vapor in soils may enhance the ability of *Larrea tridentata* to maintain photosynthesis level at lower soil water potential (Syvertsen et al., 1975) and contribute up to 40% of hourly increases in nocturnal soil moisture within the 15–35 cm layer in a seasonally dry ponderosa pine forest (Warren et al., 2011). Soil water vapor can also be transported within the soils in response to large gradients in the salt content of the soil (Kelly and Selker, 2001). In extremely dry soils, the intrusion of atmospheric vapor into the upper few centimeters of soil and its condensation can lead to biologically significant increases in liquid soil water content (Henschel and Seely, 2008).

Land-atmosphere exchange modeling has shown that including a more spatially complex and variable evapotranspiration signal relative to precipitation improves the comparison with observations (Jouzel and Koster, 1996; Yoshimura et al., 2006). Soil water vapor isotopes can help with this parameterization through a combination of measurements and modeling. Due to practical difficulties in sampling, soil evaporation isotopic composition has traditionally been

121 modeled rather than measured. The most commonly used model is the Craig-Gordon model
122 (Craig and Gordon, 1965; Horita et al., 2008) formulated to estimate equilibrium and kinetic
123 isotopic fractionation during evaporation from the ocean surface. This model has been modified
124 for various applications (Horita et al., 2008), and recently numerical models of isotope flux from
125 the soil have also been developed as alternatives to Craig-Gordon (Braud et al., 2005a; Braud et
126 al., 2009b; Haverd and Cuntz, 2010; Mathieu and Bariac, 1996; Melayah et al., 1996a).
127 Comparisons among measured and modeled values of soil evaporate isotopic composition have
128 shown significant deviations from Craig-Gordon (Braud et al., 2009a; Haverd et al., 2011;
129 Rothfuss et al., 2010). Below we describe measurement and modeling techniques, and propose a
130 modification for Craig-Gordon specific to dry soils.
131
132 2. Measurement
133 Measurements of soil water vapor isotopic composition are scarce (Braud et al., 2009b;
134 Haverd et al., 2011; Mathieu and Bariac, 1996; Rothfuss et al., 2010; Stewart, 1972; Striegl,
135 1988) due to sampling difficulties. In this section we discuss (1) general techniques for
136 measuring water vapor isotopic composition (cryogenic sampling and direct measurement), (2)
137 sampling and measuring vapor in the vadose zone, (3) estimating the isotopic composition of soil
138 evaporation flux leaving the soil surface. Table 1 lists the measurement and modeling (Section 3)
139 methods and relevant references.
140
141 2.1 Water vapor sampling and isotope analysis
142 The traditional "cold trap" sampling technique for isotope analysis of water vapor
143 involves drawing air through a tube immersed in a dry ice-alcohol mixture (for H_2O) or liquid

144 nitrogen (for H_2O and CO_2) where the water freezes (Dansgaard, 1953; Pollack et al., 1980;
145 Yakir and Wang, 1996). The method has been optimized for efficiency, bringing sampling times
146 below 15 minutes depending on the humidity level (Helliker et al., 2002), and for portability
147 (Peters and Yakir, 2010). Another recent approach has been to use a molecular sieve to trap
148 water vapor quantitatively, from which the collected sample is distilled in the laboratory (Han et
149 al., 2006). The water sample then undergoes preparation and analysis – most commonly via mass
150 spectrometry after equilibration with CO_2 for $\delta^{18}O$ determination and reduction via Zn or U for
151 $\delta^{2}H$ determination, although there are many alternative preparation and sample introduction
152 techniques, as well as new optical analytical methods available (de Groot, 2009).
153 Cryogenic sampling of atmospheric water vapor has been performed at various scales
154 since the first vertical profile collections in the 1960's over North America and Europe, which
155 included sampling in both troposphere and stratosphere (Araguas-Araguas et al., 2000; Pollack et
156 al., 1980; Rozanski, 2005). Near-surface cryogenic atmospheric water vapor sample collections
157 have been performed in Europe, Asia, Brazil, and Israel (Risi et al., 2010b; Rozanski, 2005;
158 Twining et al., 2006; Yamanaka and Shimizu, 2007; Yu et al., 2005), with one group making
159 routine collections since the early 1980s at a surface collection station in Heidelberg, Germany
160 (Jacob and Sonntag, 1991; Rozanski, 2005).
161 With the development of relatively portable laser isotope analyzers (Kerstel et al., 1999),
162 many airborne and ground-based measurements of $\delta^{18}O$ and $\delta^{2}H$ have been made (Griffis et al.,
163 2010; Hanisco et al., 2007; Lee et al., 2005; Webster and Heymsfield, 2003). The laser isotope
164 instrumentation allows for direct, rapid (1 to 10 Hz) determination of water vapor isotopic
165 composition with uncertainties approaching those of traditional mass spectrometric methods (de
166 Groot, 2009; Wang et al., 2009). There are now also remote sensing technologies that produce

water isotope data for the atmosphere (Worden et al., 2007), and ground-based Fourier Transform Infrared Spectroscopy (FTIR) is developing into a source of this information for the lower troposphere (Schneider et al., 2010).

2.2 Soil water vapor sampling and isotope analysis

Sampling of soil water vapor has been performed in the past using soil gas sampling apparatus and, as with atmospheric water vapor, cryogenic traps either in the laboratory (Stewart, 1972) or the field (Mathieu and Bariac, 1996; Striegl, 1988). The pioneering work of Zimmerman et al. (1967) on evaporative enrichment in liquid soil water isotopes includes an apparatus that directly collects the vapor resulting from soil evaporation, but this condensed vapor was not analyzed. Soil gas sampling via pumping is routinely performed during the monitoring and remediation of organic solvent contamination of the subsurface. The solvent sampling and pumping devices, however, are not designed for the high concentrations and low vapor pressures that characterize soil water vapor relative to organic solvents (e.g., trichloroethylene). However, the vadose zone modeling efforts surrounding soil gas sampling can help in estimating the area of influence for a given pumping rate and time span. For example, the USGS modeling framework MODFLOW now has a module for vadose zone gaseous transport (Panday and Huyakorn, 2008).

The main concern in sampling of soil water vapor for isotope analysis is the fractionation of the original isotopic composition through (1) inducing evaporation of the liquid soil water during sampling, and (2) condensing vapor inside the sampling apparatus due to the typically saturated conditions of soil water vapor (Campbell and Norman, 1998). An approach to reduce the risk of inducing evaporation is to pump at low flow rates (<200 mL/min), which has

produced reasonable results during initial testing (Section 4). Condensation in the sampling apparatus is reduced by minimizing tubing length, using all Teflon or high density polyethelene materials on wettable surfaces, and insulating or even heating the tubing if necessary (Griffis et al., 2010). In wet soils, various membranes could be used to exclude liquid water from the sampling apparatus up to a certain level of pore space saturation. Once the soils reach a low air-filled porosity level, however, authentic vapor sampling becomes impossible. At this critical level, which still needs to be determined empirically for each sampling method and soil type, liquid-vapor equilibrium needs to be assumed and the liquid itself analyzed. In a novel approach aimed at estimating this liquid soil water isotopic composition *in situ*, a membrane contactor (Membrana) has been shown to provide reliable results across a fairly wide soil temperature range (8-21°C) through the controlled evaporation of liquid soil water (Herbstritt et al., 2012).

There are two methods for estimating liquid soil water isotopic composition that are related to soil water vapor sampling. They involve sampling and analyzing CO_2 or water vapor that is in isotopic equilibrium with liquid soil water. The CO_2 sampling method is based on isotope equilibrium between soil CO_2 and liquid soil water (Scrimgeour, 1995), which has been shown to be complete below the depth of atmospheric CO_2 invasion into the soil surface (Wingate et al., 2009). This depth of invasion was found to be shallower than 5 cm in Mediterranean soils (Wingate et al., 2009), which is consistent with other investigations that found good agreement between liquid soil water and CO_2 at their shallowest depths – 20 cm (Tang and Feng, 2001) and 30 cm (Hesterberg and Siegenthaler, 1991). Interestingly, although the uncatalyzed equilibrium reaction between CO_2 and H_2O reaches equilibrium in about 3 hours (Dansgaard, 1953), the enzyme carbonic anhydrase acts as a catalyst in both plant leaves and in soil, such that $\delta^{18}O$ of CO_2 is a good tracer of photosynthetic and respiratory CO_2 exchange with

213 the atmosphere (Wingate et al., 2009). It is not clear whether soil water vapor plays a significant
214 role in this reaction, but a calculation by Hsieh et al. (1998) estimates the added uncertainty due
215 to reactions between different phases of water in the soil at 0.36 ‰ for $\delta^{18}O$. The sampling
216 method for CO_2 is either with a chamber placed above the soil surface (e.g., Wingate et al.,
217 2008), or a tube buried in the ground (Tang and Feng, 2001).

218 The second equilibration method involves placing a soil sample in a sealed plastic bag,
219 filling the bag with dry air, and allowing the atmosphere inside the bag to reach 100% relative
220 humidity at a constant temperature (Wassenaar et al., 2008). The bag is then punctured with a
221 syringe connected directly to a laser isotope analyzer, the vapor is analyzed directly and its
222 isotopic composition is used along with the equilibration temperature to calculate the soil liquid
223 isotopic composition. This method is instructive with respect to the rate of equilibration between
224 liquid and vapor phases – from 10 min (free water) to 3 days (clay) at 22 °C – as well as the time
225 for the laser isotope analyzer to provide a stable signal (~300 s with a flow rate of ~150 mL/min,
226 and a headspace of ~900 mL). For comparison with equilibration in the field, a study in volcanic
227 soils of Hawaii estimated an *in situ* equilibration time of 48 hrs between $\delta^{18}O$ of liquid soil water
228 and soil CO_2 (Hsieh et al., 1998). Another interesting aspect of the plastic bag equilibration
229 method is that below 5% volumetric water content, the data was apparently not useable even
230 though the headspace reached 100% relative humidity. This method is similar to direct
231 equilibration of soils and plants with CO_2 and H_2 in the laboratory (Scrimgeour, 1995), which
232 was proposed as a good method for obtaining results for very dry samples (<0.5 mL of water).

233 A comparison among CO_2 equilibration, vacuum distillation and azeotropic distillation
234 found fair agreement among the methods, but also showed distinctly poor results for the CO_2
235 method in samples drier than about 5% moisture content (Hsieh et al., 1998). The equilibration

methods for liquid soil water are potentially quite useful in studies of plant xylem and transpired water isotopic composition in that they could provide a better representation of plant-available water than vacuum and chemical distillation methods, which are performed at elevated temperatures and thus can access more tightly bound water in the soil (Araguas-Araguas et al., 1995; Hsieh et al., 1998; Walker et al., 1994). However, further studies are needed to relate soil water held at various water potentials to plant water uptake (e.g., Brooks et al., 2010), liquid-vapor equilibration times, and liquid-vapor fractionation factors.

2.3 Measuring the isotopic composition of soil evaporation

The isotopic composition of soil evaporation can be estimated through sampling water vapor above the soil. Measurements of the near-surface atmosphere have been used for this purpose to measure vapor efflux from terrestrial ecosystems, including the "Keeling Plot" approach using gradients in isotopic composition and bulk concentration of CO_2 (Keeling, 1958), which has also been applied to water vapor (Wang et al., 2010; Yakir and Sternberg, 2000; Yepez et al., 2003). Additional methods include the Flux Gradient (Griffis et al., 2004; Yakir and Wang, 1996) and Eddy Covariance techniques (Griffis et al., 2010; Lee et al., 2005). Each of these methods involves making measurements at some altitude above the ground surface, and thus their results are applicable to a certain horizontal "footprint" from which the vapor originated. If this footprint is unvegetated, then the water vapor flux signal can be completely attributed to soil evaporation. If there is some vegetation present, however, the measured flux is from the combined evapotranspiration. Decomposing this combined signal is possible (Haverd et al., 2011; Rothfuss et al., 2010; Wang et al., 2010), but the assumptions involved in estimating the transpiration and evaporation end-members currently lead to a high degree of uncertainty.

Specifically, the isotopic end-member for transpiration represents an integrated signal weighted by the amount of transpired water delivered by each root of each transpiring plant with the active flux footprint. If the mean rooting depth changes (e.g., grasses become active), the transpiration end-member will change. Thus, characterizing this end-member through time requires regular measurement of soil water isotopic composition profiles in a way that captures heterogeneity across the footprint, as well as measurement of transpiring leaf area for plant groups with differing rooting depths (e.g., grasses, shrubs, trees). Numerical models of soil evaporation isotopic composition, discussed below, coupled with land surface dynamic models have made some advances in this field (Braud et al., 2009a; Haverd et al., 2011).

Another method for measuring soil efflux involves placing a sealed chamber over the soil, and measuring the vapors that move up into the chamber (Haverd et al., 2011; Wingate et al., 2008). The issues with this type of measurement include making a good seal with the soil surface to avoid drawing in atmospheric air, and altering the ambient conditions of the soil. If these sources of error can be minimized, chamber methods have the potential to provide good point estimates of CO_2 and H_2O releases from the soil. Chamber measurements are still challenging, however, as they necessarily change the ambient conditions, especially with respect to wind velocities and concentration gradients for the gases of interest. Improvements are still being made, particularly with open-chamber methods (Midwood et al., 2008) and open-path isotopic composition sensors (Humphries et al., 2010).

However, point estimates either with chamber methods, sampling, or *in situ* measurements, must be viewed with caution given the typically large degree of heterogeneity in a soil landscape (Ogée et al., 2004). For this reason, integrated landscape-scale estimates of soil evaporation will be more useful for investigating overall ecosystem functioning. Thus increasing

the size of an atmospheric measurement's footprint can increase its relevance for scaling up to regional and global levels. The next step towards understanding the distribution of soil evaporation isotopic composition across a wider range of temporal and spatial scales is modeling based on more readily available data (Braud et al., 2009a; Haverd et al., 2011) and improved mechanistic understanding (e.g., the effect of water potential on soil evaporation isotopic composition as proposed in this paper, Equation 9).

3. Modeling soil water vapor isotopic composition

Modeling efforts relating to soil water vapor isotopic composition (δ_V) have focused on estimating the isotopic composition of soil evaporation (δ_E), with reference to the fractionation that occurs during the evaporation of liquid soil water (δ_L). The δ_E modeling has typically been performed in the framework of open-water evaporative fractionation developed by Craig and Gordon (1965), and recently numerical isotope transport models have been developed as an alternative (Braud et al., 2009a; Braud et al., 2005a; Haverd and Cuntz, 2010; Mathieu and Bariac, 1996; Melayah et al., 1996a; Shurbaji and Phillips, 1995). Here we present a discussion of (1) equilibrium isotope fractionation between liquid and vapor forms of water from theoretical and empirical perspectives, (2) evaporative fractionation and the Craig-Gordon (CG) model, and (3) soil water vapor isotope models including modified CG and isotope transport models.

3.1 Liquid-vapor equilibrium isotopic fractionation

Every isotope fractionation model relies on estimates of the liquid-vapor equilibrium fractionation factors ($\alpha_{e,L/V}(^{18}O)$ and $\alpha_{e,L/V}(^{2}H)$; Equation 1), and how this parameter changes under different environmental conditions. Temperature is the environmental parameter used for

305 the $\alpha_{e,L/V}$ estimates, and this relationship ($\alpha_{e,L/V}$-T) has been well characterized experimentally
306 (Horita and Wesolowski, 1994; Majoube, 1971). Efforts to model the underlying processes of the
307 $\alpha_{e,L/V}$-T relationship from theory (Chialvo and Horita, 2009; Oi, 2003) have not improved on the
308 empirical relationships that have been implemented in studies of evaporation for more than four
309 decades (Horita et al., 2008). Thermodynamic modeling based on Equations of State for various
310 water molecule isotopoloques, captures the purely empirical relationships well (Japas et al.,
311 1995; Polyakov et al., 2007). The $\alpha_{e,L/V}$-T relationship has only been modified slightly since
312 (Majoube, 1971) to cover a larger temperature range (Horita and Wesolowski, 1994), with the
313 current formulations given in Equations 2 and 3.
314
315 $$\alpha_{e,L/V}(^{18}O) = \frac{^{18}R_L}{^{18}R_V} \qquad \text{[Equation 1]}$$
316 $$10^3 \ln \alpha_{e,L/V}(^{18}O) = -7.685 + 6.7123\left(\frac{10^3}{T}\right) - 1.6664\left(\frac{10^6}{T^2}\right) + 0.35041\left(\frac{10^9}{T^3}\right) \qquad \text{[Equation 2]}$$
317 $$10^3 \ln \alpha_{e,L/V}(^{2}H) = 1158.8\left(\frac{T^3}{10^9}\right) - 1620.1\left(\frac{T^2}{10^6}\right) + 794.84\left(\frac{T}{10^3}\right) - 161.04 + 2.9992\left(\frac{10^9}{T^3}\right)$$
318 [Equation 3]
319
320 Three modeling approaches using (1) molecular simulation, (2) theoretical ("*ab initio"*)
321 calculations and (3) thermodynamics have recently been compiled to examine the effects of
322 isotopic substitutions on the properties of the water molecule (Chialvo and Horita, 2009). These
323 three approaches capture the shape of the observed $\alpha_{e,L/V}$-T relationships (Equations 2 and 3), but
324 the difference among the models is large relative to the level of fractionation seen empirically
325 (Table 2). Molecular modeling is used by chemists as a supplement to experimentation in an

effort to understand the underlying dynamics in chemical reactions. Various modeling approaches are used to depict electron densities and molecular orbital dynamics based on energies associated with all bonded and non-bonded atomic interactions.

Using molecular-based simulation, $\alpha_{e,L/V}$ was estimated based on two contrasting models of the water molecule: Gaussian charge polarizable (GCP) and nonpolarizable extended simple point charge (SPC/E). The GCP model performed better than SPC/E, but produced fractionation factors ($\alpha_{e,L/V}$) around 5 ‰ higher for $\alpha_{e,L/V}(^{18}O)$ and 500 ‰ higher for $\alpha_{e,L/V}(^{2}H)$ than those $\alpha_{e,L/V}$ values found experimentally at 25 ºC (Horita and Wesolowski, 1994; Majoube, 1971). Chialvo and Horita (2009) recognized the large deviations of their models from experimental data, and suggested a parameterization of their $\alpha_{e,L/V}$-T relationship that will allow for experimental data to create more accurate molecular dynamics models in the future. Two *ab initio* ("from first principles") models using molecular orbital calculations performed somewhat better relative to empirical data, within 4 ‰ for $\alpha_{e,L/V}(^{18}O)$ and 66 ‰ for $\alpha_{e,L/V}(^{2}H)$ (Oi, 2003).

Lastly, two thermodynamic modeling efforts produced much better results applying solute dissolution (Japas et al., 1995) and corresponding states principle (Polyakov et al., 2007) approaches, apparently with deviations from empirical data of less than 0.1 ‰ and 1 ‰ for $\alpha_{e,L/V}(^{18}O)$ and $\alpha_{e,L/V}(^{2}H)$, respectively, at typical environmental temperatures. Despite their different approaches, these two thermodynamic models show very good agreement with each other, especially below 50 °C. These approaches do incorporate some empirical data – e.g., vapor pressures for solutions of pure isotopically substituted water (D_2O and $H_2{}^{18}O$).

Overall, the somewhat empirical thermodynamic modeling (Japas et al., 1995; Polyakov et al., 2007) performed much better than the purely theoretical *ab initio* (Oi, 2003) and molecular simulation (Chialvo and Horita, 2009) models. Most importantly, all three approaches, in spite of

drastic differences in $\alpha_{e,L/V}$, show the same shape and limit characteristics. Therefore these models have the potential to provide insight into the underlying mechanisms of the robust empirical $\alpha_{e,L/V}$-T relationships (Equations 2 and 3), which are still preferred for estimating $\alpha_{e,L/V}$ (Gat, 1996; Horita et al., 2008; Kim and Lee, 2011).

3.2 Isotopic fractionation during evaporation from free water

The empirical $\alpha_{e,L/V}$ values discussed above can be used to calculate the isotopic composition of vapor that is in isotopic equilibrium with liquid water at a given temperature. This equilibrium is most likely reached in soil pore spaces where sufficient moisture is available (Braud et al., 2005a; Braud et al., 2005b; Mathieu and Bariac, 1996), as is illustrated with a case study in Section 4. The fractionation during evaporation from a free surface (e.g., the ocean), involves both equilibrium (α_e) and kinetic (α_k) fractionation, and will be described here as a basis for the soil evaporation discussion that follows.

Modeling efforts that include both equilibrium and kinetic fractionation were motivated by early observations of marine water vapor being isotopically depleted relative to the equilibrium fractionation factor for a given temperature (Craig and Gordon, 1965). Thus, in addition to $\alpha_{e,L/V}$ for a given temperature at the evaporating surface (T_0), the parameters required for the estimation of the kinetic fractionation include relative humidity (h), diffusivity ratios of the isotopologues of interest (D/D_i), and an aerodynamic parameter (n, Table 3). The variability in these kinetic parameters is dominated by relative humidity of the air into which the water is evaporating (h_A), which must be recalculated (h_A') from the measured value at some height above the evaporating surface based on the temperature and activity of water at the evaporating surface (Craig and Gordon, 1965; Horita, 2005; Horita et al., 2008; Sofer and Gat, 1975). The overall

372 relationship (Equations 4, 5 and 6) was first described by Craig and Gordon (1965) and is still
373 used to estimate isotopic fractionation during evaporation from both a free surface and soil (Gat,
374 1996; Horita et al., 2008), with modifications specific to soil evaporation described in the next
375 section. As summarized in Horita et al. (2008), the CG model is a physically-based model where
376 the air-water interface is at isotopic equilibrium. Above this interface is a laminar flow layer of
377 variable thickness, which accounts for additional fractionation due to differences in molecular
378 diffusivities of isotopologues. This laminar layer is followed by a turbulent mixing layer, which
379 does not contribute to isotope fractionation.
380
381 $$\delta_E = \frac{\delta_L / \alpha_{e,L/V} - h_A^{'}\delta_A - (\alpha_{e,L/V} - 1) - \varepsilon_{k,L/V}}{1 - h_A^{'} + \varepsilon_{k,L/V}} \quad \text{[Equation 4]}$$
382 $$\varepsilon_{k,L/V} = n(1 - h_A^{'})\left(\frac{D}{D_i} - 1\right)\frac{r_m}{r} \quad \text{[Equation 5]}$$
383 $$h_A^{'} = \frac{h_A e_{sA}}{a_w e_{s0}} \quad \text{[Equation 6]}$$
384
385 The "weighting term" r_m/r is assumed to be 1 for small water bodies, but can reach 0.5 for
386 strongly evaporating systems like the Mediterranean Sea (Gat, 1996). The effect of the
387 aerodynamic parameter n (n = 0.5 for free water, 1 for completely laminar flow as in very dry
388 soil, see below) is to reduce the kinetic fractionation due to the reduced role of molecular
389 diffusion when the turbulent layer interacts strongly with the evaporating surface. Higher
390 humidity leads to reduced kinetic fractionation, but its overall effect on δ_E is not straightforward
391 because an increased h_A' leads to both a lower numerator and a lower denominator in Equation 4.
392 Interestingly, the thermodynamic activity of water (a_w, between ~0.6 in brines to 1 in fresh

393 water) acts to increase the normalized humidity h_A' for evaporation from saline water. The same
394 is true for evaporation from soils, as introduced below (Equation 9), when soil water potential is
395 used to calculate the activity of soil water. Thus, a reduced activity of water leads to limited
396 evaporative enrichment in saline water relative to fresh water exposed to the same conditions
397 (Horita, 2005). The necessary field measurements to make a CG calculation are discussed with
398 the case study in Section 4. The appropriate height for making the atmospheric measurements is
399 above the turbulent mixing layer, given that these values are meant to represent "free
400 atmosphere" (Craig and Gordon, 1965; Horita et al., 2008), although this condition is most likely
401 not fully satisfied for many applications of the CG model.
402 In addition to normalized humidity, the representation of diffusive fractionation has a
403 great effect on δ_E modeled from CG (Braud et al., 2009a). Cappa et al. (2003) provided
404 significantly revised diffusivities of water isotopologues (D/D_i in Equation 7, Table 2) based on
405 gas kinetic theory as well as experimental results, and emphasize the use of skin temperature
406 rather than bulk temperature for fractionation calculations. However, evidence for surface
407 cooling during evaporation from natural water bodies is not yet available. Thus, the diffusivities
408 of Merlivat (1978) are still generally preferred (Lee et al., 2007). Recent evaluations and
409 experimental results from Luz et al. (2009) have also suggested that the Merlivat (1978) values
410 are still valid. However, if an evaporating body is not well mixed, lower temperatures apparently
411 do develop in the top 0.5 mm, and if this temperature structure persists, Cappa et al. (2003)
412 clearly showed that diffusivities and associated kinetic fractionation factors can be quite different
413 from those calculated based on the temperature of the bulk water. This enhanced fractionation
414 may be counteracted by the accumulation of enriched isotopologues at the surface, given the lack
415 of mixing required for significant surface cooling to occur (Horita et al., 2008).

416

417 3.3 Modeling the isotopic composition of soil water vapor and soil evaporation

418 Due to the difficulty in soil water vapor isotope (δ_V) sampling in the past, there is little
419 information on δ_V directly collected from soil profiles (Mathieu and Bariac, 1996). Direct
420 measurements of *in situ* soil water vapor δ_V are now possible and will provide a direct check for
421 the utilization of the CG model in various conditions especially for dry soils. An important
422 missing component in the application of the CG model to soil evaporation is the effect of water
423 potential on the activity of water, which can be easily incorporated with measurements of soil
424 moisture or soil water potential, as developed below.

425 In recent years, transport-based isotope models such as SiSPAT-isotope model (Braud et
426 al., 2009a; Braud et al., 2005a) and Soil-Litter-Iso model (Haverd and Cuntz, 2010; Haverd et
427 al., 2011) have been developed to model soil δ_E, building from analytical solutions for idealized
428 cases that were developed previously (Barnes and Allison, 1983). The Soil-Litter-Iso model was
429 compared with other analytical frameworks (Haverd and Cuntz, 2010), and recent testing of the
430 model against water vapor isotopic composition data from a chamber placed on top of the soil
431 yielded very promising results. The model captures diurnal patterns and a 10-day dry-down quite
432 well, although a mean deviation of around 10 ‰ was observed for δ^2H between measured and
433 modeled values (Haverd et al., 2011). SiSPAT-isotope model was tested using laboratory column
434 setup and parameters were calibrated to maximize the model-data agreements. The results
435 indicate that the evaporative enrichment process is very sensitive to changes in kinetic
436 fractionation (Braud et al., 2009a).

437 The numerical models have introduced many important soil parameters such as the soil
438 moisture, tortuosity, and water potential, which are not explicitly considered in the CG modeling

framework. The effect of these parameters could be lumped into the kinetic isotope fractionation factor (α_k) to improve the agreement between model output and observational data for each time step and soil layer in the model. The missing key component to test these effects is the direct measurement of δ_E and authentic δ_{SV} measurements. The mass-balance framework developed in Wang et al. (2012) for direct and continuous quantification of the isotopic composition of leaf transpiration could be adopted for quantifying soil δ_E from measurements, which then can be verified using authentic *in situ* soil water vapor δ_V measurements.

The surface boundary condition of the most recent bare soil evaporation numerical model provides an isotope evaporative flux based on equilibrium (α_e) and kinetic fractionation (α_k) factors, as well as heat and moisture conservation equations solved for the soil-air interface (Haverd and Cuntz, 2010). The α_k calculation involves adjusting the molecular diffusivity ratio of isotopologues by the aerodynamic parameter *n* (Equation 7), analogous to Equation 5.

$$\alpha_{k,L/V} = \left(\frac{D_i}{D}\right)^n \qquad \text{[Equation 7]}$$

This equation has taken on various forms in models, as summarized and evaluated by Braud et al. (2005b). In an attempt to incorporate the laminar flow development of the soil as it dries, n is related to volumetric soil moisture (θ) as first proposed by Mathieu and Bariac (1996) and adopted in subsequent numerical models (Braud et al., 2009a; Braud et al., 2005b; Haverd and Cuntz, 2010). This relationship (Equation 8) allows for *n* to vary between 0.5 for saturated conditions and 1 for dry soil ("residual" soil moisture) where the laminar layer will have fully developed.

$$n = \frac{(\theta_0 - \theta_r)n_a + (\theta_s - \theta_0)n_s}{\theta_s - \theta_r} \quad \text{[Equation 8]}$$

Where $n_a = 0.5$ and $n_s = 1$, and subscripts *s*, *r*, and *0* refer to saturated, residual and ambient conditions at the evaporating surface, respectively. In the original formulation θ_r was defined as the minimum soil moisture reached when the soil is in equilibrium with the atmosphere (Mathieu and Bariac, 1996).

The numerical models also include the humidity of the soil modeled from soil water potential as part of their evaporative flux formulation (Braud et al., 2009a; Braud et al., 2005a; Mathieu and Bariac, 1996). However, they do not take into account the relationship between water potential and the activity of the water, a_w, which is provided by the Kelvin equation (Equation 9; Barnes and Gentle, 2011; Gee et al., 1992).

$$\ln(a_w) = \frac{\psi_0 M_w}{R T_0 \rho_w} \quad \text{[Equation 9]}$$

where ψ_0 is soil water potential [kPa] of the evaporating surface, M_w is the molecular weight of water (18.0148 [g mol^{-1}]), R is the ideal gas constant (8.3145 [mL MPa mol^{-1} K^{-1}]), ρ_w is the density of water, and T_0 is the temperature [K] of the evaporating surface.

The activity of water is equivalent to the relative humidity in the soil under liquid-vapor equilibrium, a relationship that is commonly used to measure water potential in soils through devices that measure the dew point in a sealed chamber that contains a soil sample (Gee et al., 1992). When considered with the CG model framework, a reduction in a_w increases the

normalized humidity h_A' (Equation 6), reducing $\varepsilon_{k,L/V}$ (Equation 5), ultimately affecting the δ_E calculation (Equation 4). This modification of h_A' is identical to the normalization using the activity of water in saline waters (Horita et al., 2008). Thus, it can be easily incorporated into CG formulations by combining Equations 6 and 9. The effect of including the water potential in a CG model calculation of δ_E is illustrated with measurements of a soil profile at Mpala Research Center, Kenya described in Section 4 below.

In addition to the effects of water potential on fractionation during evaporation, the relationship between equilibrium fractionation in soils and water potential has yet to be rigorously described. There are strong indications from the equilibration of CO_2 with soil water that dry soils exhibit a different equilibrium behavior than wet soils (Hsieh et al., 1998; Wassenaar et al., 2008). In reviewing some field collections of soil water vapor, Mathieu and Bariac (1996) commented that in dry soils the observed vapor was more enriched than would be expected from equilibrium fractionation at the given temperature. Changes in water structure and properties such as vapor pressure due to confinement in small spaces such as soil pores have been recently reported for bulk water in carbon nanotubes (Chaplin, 2010) and for hydrogen isotopes in water adsorbed to porous silica tubes, leading to significant differences in equilibrium isotope fractionation between liquid and vapor phases (Richard et al., 2007).

An interesting early experiment on water isotopic fractionation in clays (Stewart, 1972) used a saturated KCl solution as the moisture source for vapor that was allowed to equilibrate with a thin layer of dried clay. In this KCl-vapor-clay system, a wide range of isotopic fractionation factors was observed ($\alpha_{L/V}(^2H)_{clay}$ = 0.93 to 1.06, with a median of 1.04; HDO concentration ratios of Stewart (1972) were divided by the estimated $\alpha_{L/V}(^2H)_{KCl}$ = 1.06). The temperatures weren't controlled, and a value of $\alpha_{L/V}(^2H)_{KCl}$ as low as 1.06 would require a

506 temperature >40 ºC using Equation 3 (Horita and Wesolowski, 1994). Nevertheless, the
507 indication is that $\alpha_{L/V}(^2H)_{clay}$ can have a wide range, but with values below the isotopic
508 fractionation factor for free water at a given temperature. Interestingly, the recent analogous
509 work with porous silica tubes instead of clays (Richard et al., 2007) found $\alpha_{L/V}(^2H)$ values of
510 around 1.03 at 20 % relative humidity and 1.05 at 80 % relative humidity at around 20 ºC,
511 compared with 1.085 from Equation 3. Thus, these results are somewhat consistent with the less-
512 controlled early study with clays, suggesting that the equilibrium isotopic fractionation between
513 vapor and water adsorbed on clays is lower than the free water value at the same temperature.
514 A final consideration towards understanding the isotopic composition of soil water vapor
515 is the organization of water molecules within the liquid phase. It has been shown that enriched
516 isotopologues exist at higher concentrations near dissolved ions, and thus near particle surfaces
517 (Phillips and Bentley, 1987). Given this structure, there could potentially be a concentration of
518 depleted isotopes near the evaporating surface of porewater. This "hydration sphere isotope
519 effect" would cause isotopic differences between bulk water and the evaporating surface and
520 require a stagnant solution, similar to the skin temperature effect shown by Cappa et al. (2003).
521 The impact of isotopic gradients within individual pockets of liquid soil water on δ_E has not been
522 explored. If an isotopic difference exists between bulk water and the evaporating surface, this
523 could be another reason to use equilibration analytical methods on undisturbed soils for
524 estimating liquid isotopic composition (Herbstritt et al., 2012; Hsieh et al., 1998; Scrimgeour,
525 1995; Wassenaar et al., 2008).
526 The isotopic composition of soil evaporation is the result of several different fractionation
527 processes. First, the phase change and equilibrium processes within the soil matrix are governed
528 by temperature and soil water potential. Kinetic fractionation is affected by physical

529 characteristics of the diffusion path (e.g. tortuosity) as well as isotopic gradients between the site
530 of evaporation and the initiation of turbulent mixing just above the soil surface. Vapor moving
531 vertically through the soil will also likely re-equilibrate with the liquid water along its path. The
532 overall apparent fractionation between liquid water at any given depth and the resultant
533 evaporative flux leaving the soil surface reflects all of these fractionation processes. As the liquid
534 water sources for soil evaporation fluctuate in depth and isotopic composition, modeling the soil
535 evaporation isotopic end-member accurately at any given time becomes very difficult. Thus,
536 techniques for measuring the evaporated vapor itself will be very important as this field moves
537 forward. In the next section we provide an example of one step in this direction: direct
538 measurements within the soil matrix.
539
540 4. Case Study: Soil water vapor in an African savanna
541 An example of direct soil water vapor isotope measurement is shown in Figure 1, with
542 data from a single profile collected at Mpala Research Centre, Kenya, on 29 March 2011 from
543 12:45 to 13:00 local time. The soil is a red sandy loam with a bulk density of 1.45 [g cm^{-3}] and a
544 porosity of 0.45. The vegetation is mixed semi-arid savanna, and the local mean annual
545 precipitation is around 600 mm. Soil vapor was sampled at four depths (5, 10, 20 and 30 cm;
546 sampled in depth order starting with 5 cm) via buried Teflon tubing, with the final 10 cm of each
547 tube perforated and packed with glass wool. Soil vapor was drawn directly into a laser water
548 vapor isotope analyzer (DLT100, Los Gatos Research Inc., Mountain View, CA) at a flow rate of
549 150-180 mL/min, diluted with ambient air (intake at 2 m above ground) for a total flow of 400
550 mL/min. This dilution allowed for reduced flow rates at the soil vapor intakes and lowered the
551 humidity in the tubing and analytical equipment to reduce the chance of forming condensation.

552 Data was collected for around 90 seconds at each depth. Soil temperature was measured with
553 TCAV averaging soil temperature probes (Campbell Scientific Inc., Logan, UT) at 5 and 20 cm,
554 and a linear profile was assumed for 10 and 30 cm. Ambient atmospheric water vapor isotopic
555 composition, humidity and temperature were sampled at 2 m above the ground surface. Soil
556 samples were collected from an auger hole adjacent to the buried tubing immediately after vapor
557 sampling. Water potential was measured via a dew point potentiometer (WP4T, Decagon
558 Devices Inc., Pullman, WA). Liquid soil water was isolated via cryogenic vacuum distillation
559 (West et al., 2006) and analyzed with a continuous-flow water vapor isotope analyzer using a
560 heated nebulizer for sample introduction (WVISS, Los Gatos Research, Inc.).
561 Equilibrium water vapor isotopic compositions were calculated for each depth based on
562 the respective measured liquid soil water isotopic composition, soil temperature and the
563 associated fractionation factors (Equations 1 to 3). For each depth, the corresponding CG
564 modeled values were calculated in two ways: (1) conventionally, using Equations 2 to 8
565 assuming a_w=1 (Figure 1 and Table 3, $\delta_E\ (\theta,T)$); (2) including soil water potential by calculating
566 a_w with Equation 9 ($\delta_E\ (\theta,T,\psi)$). The parameters for CG calculations are given in Table 3 with
567 specific examples and typical ranges.
568 The measured soil vapor isotope values fell close to those that would be expected for
569 isotopic equilibrium at the temperature for each depth (Figure 1). The measured values cover a
570 reduced range (-4.0 to -2.2 ‰ for $\delta^{18}O$) relative to the equilibrium values (-7.5 to 4.1 ‰ for
571 $\delta^{18}O$), but have similar mean values of -2.8 ‰ and -3.0 ‰ for $\delta^{18}O$ and -57 ‰ and -65 ‰ for
572 $\delta^{2}H$, respectively. These mean values are weighted by soil moisture contents (θ_0) of 5.3, 6.0, 6.2,
573 and 6.6 vol% for 5, 10, 20 and 30 cm, respectively. The fact that the measured vapor isotope
574 values fall in a smaller range, but within the calculated equilibrium values, suggests that either

575 the sampling process induced mixing of vapor from various depths, or that the vapor is
576 somewhat mixed within the sampling depths at this time of day. Sampling-induced mixing is
577 likely given that around 0.5 to 0.6 L of soil were influenced by the sampling at each depth.
578 Subtracting volumetric water contents from a porosity of 0.45 gives air-filled porosity values of
579 0.38 to 0.39, resulting in a radius of influence of about 7 cm around each perforated section of
580 tubing, suggesting that the sampling depths overlap to some degree. The three sets of values –
581 liquid, measured vapor and equilibrium vapor – have similar slopes of 3.1, 3.4, and 3.0 (δ^2H vs.
582 $\delta^{18}O$). Although this level of consistency among slopes is encouraging within the scope of the
583 present study, a second study is needed to examine the differences in these slopes relative to
584 differences in fractionation factors as well as the combined uncertainties in δ^2H and $\delta^{18}O$.
585 Interestingly, the measured soil water vapor isotope values are much closer to the equilibrium
586 vapor isotope values than the CG modeled δ_E values (Figure 1). This example is therefore
587 consistent with the typical assumption of isotopic equilibrium between liquid and vapor in the
588 soil (e.g., Mathieu and Bariac, 1996).

589 The effect of including water activity (i.e., soil water potential, ψ) in the CG calculations
590 depends on the relationships among equilibrium vapor, ambient vapor, and ambient humidity. To
591 examine these relationships as well as the effect of including soil water content (θ), we made a
592 series of CG calculations starting with the 5 cm depth parameters of Figure 1 and Table 3. We
593 varied ψ_0 and calculated θ_0 using a relationship of the form:

594

595 $$\theta = \left(\frac{a}{-\psi}\right)^{1/b} \qquad \text{[Equation 10]}$$

596

where a = 0.00109 and b = 3.46, based on 410 paired measurements of ψ and θ for 14 separate drying experiments. The measured values ranged from -0.2 MPa to -61 MPa for ψ and 1 vol% to 41 vol% for θ.

We then calculated δ_E using Equations 2 to 9 (Figure 2, solid black lines). We also varied three atmospheric parameters T_A, δ_A and h_A (Figure 2, dashed black lines). Lastly, we made the same calculations without considering θ (i.e., n = 1) or ψ (i.e., a_w = 1), and used both conventional (Merlivat, 1978) and revised (Cappa et al., 2003) values for equilibrium isotope fractionation factors (Figure 2, gray lines). From these calculations it is clear that for drying soils, the effect of including ψ can be similar to or greater than the effect of including θ (i.e., changing n from 0.5 to 1). Including θ (Equation 8), which leads to n=0.5 in the wettest soils (θ_0 close to 0 MPa), leads to more enriched δ_E values in wetter soils. Including ψ (Equation 9) apparently leads to the opposite effect, with more enriched δ_E values in drier soils. Both mechanisms can be correct, with the former (lower n and higher δ_E in wetter soils) describing the decrease in kinetic fractionation as the soil evaporation becomes more controlled by atmospheric turbulence than by diffusion in the soil (Mathieu and Bariac, 1996). The latter (higher h_A' and higher δ_E in drier soils) simply describes the effect of lower water activity on the saturation vapor pressure in the soil. This soil water potential effect can also be as large as the impact of using the drastically different diffusivity ratios of Cappa et al. (2003) rather than those of (Merlivat, 1978).

5. Conclusions

We summarized all the available modeling and field methods to quantify isotopic composition of water vapor, with a focus on the Soil-Plant-Atmosphere Continuum. When

620 applying the Craig-Gordon (CG) modeling framework to soil evaporation, we suggest the
621 inclusion of soil water potential in the normalization of "free atmosphere" humidity to the
622 evaporating surface (Equations 6 and 9), just as water activity is included in the normalization
623 for evaporation from saline waters. This will reduce the total fractionation for evaporation from
624 unsaturated soils as predicted by the CG model. Such a reduction is consistent with observations
625 of enriched soil water vapor, and can be significant in soils with water potentials drier than
626 around -10 MPa. This improvement is easily implemented in all CG formulations, and the only
627 additional measurement required is soil water potential. This parameter can also be calculated
628 from soil water content using an appropriate soil water retention curve. There is also a possibility
629 that leaf water potential could be used to improve the use of normalized humidity in application
630 of the CG model to evaporative isotopic enrichment in leaves (e.g., Cuntz et al., 2007), although
631 leaf water potential is highly variable and more difficult to estimate than soil water potential.
632 Another feature of isotopic fractionation in soil water that is likely to change through
633 experimentation is the equilibrium fractionation factor. The equilibrium fractionation for free
634 water is still represented empirically. The indication from experiments between vapor and water
635 adsorbed onto clay and silica tubes is that liquid-vapor equilibrium fractionation is substantially
636 reduced in a porous media setting relative to free water. The structure of water changes in
637 confined spaces, and it is expected that the nature of pore spaces in different types of soils will
638 lead to different equilibrium fractionation factors. The use of stable isotopes of water vapor in
639 understanding the Soil-Plant-Atmosphere Continuum at various scales depends on an accurate
640 understanding of fractionation processes and the associated modeling of isotopic fluxes in the
641 environment. The relatively new analytical capabilities for water vapor isotopes coupled with

642 novel sampling approaches under development will provide the necessary data to follow these
643 fractionation processes *in situ*.
644

645 Acknowledgements

646 This project was funded by NSF through a CAREER award to K. K. Caylor (EAR847368). Lixin
647 Wang also acknowledges the financial support from the vice-chancellor's postdoctoral research
648 fellowship at the University of New South Wales. We greatly appreciate the field and laboratory
649 assistance of Ekomwa Akuwam, John Maina Gitonga and the staff at Mpala Research Centre.
650

651 References

652 Abramova, M.M. 1969. Movement of moisture as liquid and vapor in soils of semi-deserts. In: P.
653 E. Rytema and H. Wassink, editors, Wageningen Symposium on Water in the
654 Unsaturated Zone. IASH-UNESCO, Gentbrugge - Paris. p. 781-789.
655 Allison, G.B. and C.J. Barnes. 1983. Estimation of Evaporation from Non-Vegetated Surfaces
656 Using Natural Deuterium. Nature 301: 143-145.
657 Araguas-Araguas, L., K. Froehlich and K. Rozanski. 2000. Deuterium and oxygen-18 isotope
658 composition of precipitation and atmospheric moisture. Hydrological Processes 14: 1341-
659 1355.
660 Araguas-Araguas, L., K. Rozanski, R. Gonfiantini and D. Louvat. 1995. Isotope Effects
661 Accompanying Vacuum Extraction of Soil-Water for Stable-Isotope Analyses. Journal of
662 Hydrology 168: 159-171.
663 Barnes, C.J. and G.B. Allison. 1983. The distribution of deuterium and ^{18}O in dry soils 1.
664 Theory. Journal of Hydrology 60: 141-156.
665 Barnes, C.J. and G.B. Allison. 1988. Tracing of Water-Movement in the Unsaturated Zone Using
666 Stable Isotopes of Hydrogen and Oxygen. Journal of Hydrology 100: 143-176.
667 Barnes, G. and I. Gentle. 2011. Introduction to Interfacial ScienceOxford University Press,
668 Oxford.
669 Bittelli, M., F. Ventura, G.S. Campbell, R.L. Snyder, F. Gallegati and P.R. Pisa. 2008. Coupling
670 of heat, water vapor, and liquid water fluxes to compute evaporation in bare soils. Journal
671 of Hydrology 362: 191-205.

672 Braud, I., T. Bariac, P. Biron and M. Vauclin. 2009a. Isotopic composition of bare soil
673 evaporated water vapor. Part II: Modeling of RUBIC IV experimental results. Journal of
674 Hydrology 369: 17-29. doi:10.1016/j.jhydrol.2009.01.038.
675 Braud, I., T. Bariac, J.-P. Gaudet and M. Vauclin. 2005a. SiSPAT-Isotope, a coupled heat, water
676 and stable isotope (HDO and H218O) transport model for bare soil. Part I. Model
677 description and first verifications. Journal of Hydrology 309: 277-300.
678 Braud, I., T. Bariac, M. Vauclin, Z. Boujamlaoui, J.-P. Gaudet, P. Biron, et al. 2005b. SiSPAT-
679 Isotope, a coupled heat, water and stable isotope (HDO and H218O) transport model for
680 bare soil. Part II. Evaluation and sensitivity tests using two laboratory data sets. Journal
681 of Hydrology 309: 301-320.
682 Braud, I., P. Biron, T. Bariac, P. Richard, L. Canale, J.P. Gaudet, et al. 2009b. Isotopic
683 composition of bare soil evaporated water vapor. Part I: RUBIC IV experimental setup
684 and results. Journal of Hydrology 369: 1-16. doi:10.1016/j.jhydrol.2009.01.034.
685 Brooks, J.R.e., H.R. Barnard, R. Coulombe and J.J. McDonnell. 2010. Ecohydrologic separation
686 of water between trees and streams in a Mediterranean climate. Nature Geoscience 3:
687 100-104, doi:110.1038/ngeo1722.
688 Brunel, J.P., H.J. Simpson, A.L. Herczeg, R. Whitehead and G.R. Walker. 1992. Stable isotope
689 composition of water vapor as an indicator of transpiration fluxes from rice crops. Water
690 Resources Research 28: 1407-1416.
691 Campbell, G.S. and J.M. Norman. 1998. An introduction to environmental biophysicsSpringer,
692 New York.
693 Cane, G. and I.D. Clark. 1999. Tracing ground water recharge in an agricultural watershed with
694 isotopes. Ground Water 37: 133-139.

695 Cappa, C.D., M.B. Hendricks, D.J. DePaolo and R.C. Cohen. 2003. Isotopic fractionation of
696 water during evaporation. Journal of Geophysical Research 108: 4525.
697 Chaplin, M.F. 2010. Structuring and behavior of water in nanochannels and confined spaces. In:
698 L. J. Dunne and G. Manos, editors, Adsorption and Phase Behavior in Nanochannels and
699 Nanotubes. Springer, New York. p. 241-255.
700 Chialvo, A.A. and J. Horita. 2009. Liquid-vapor equilibrium isotopic fractionation of water: How
701 well can classical water models predict it? The Journal of Chemical Physics 130: 094509.
702 Coplen, T.B. 2011. Guidelines and recommended terms for expression of stable isotope-ratio and
703 gas-ratio measurement results. Rapid Communications in Mass Spectrometry 25: 2538-
704 2560.
705 Craig, H. 1961. Isotopic variations in meteoric waters. Science 133: 1702-1703.
706 E. Tongiorgi. 1965. Deuterium and oxygen-18 variations in the ocean and marine atmosphere.
707 Stable isotopes in oceanographic studies and paleotemperatures, Pisa. Laboratory of
708 Geology and Nuclear Science.
709 Cuntz, M., J. Ogée, G. Farquhar, P. Peylin and L.A. Cernusak. 2007. Modelling advection and
710 diffusion of water isotopologues in leaves. Plant Cell and Environment 30: 892-909.
711 D'Odorico, P., K. Caylor, G.S. Okin and T.M. Scanlon. 2007. On soil moisture-vegetation
712 feedbacks and their possible effects on the dynamics of dryland ecosystems. Journal of
713 Geophysical Research 112: G04010.
714 Dansgaard, W. 1953. The abundance of ^{18}O in atmospheric water and water vapor. Tellus 5: 461-
715 469.
716 Dawson, T.E. 1993. Hydraulic Lift and water-use by plants: Implications for water-balance,
717 performance and plant-plant interactions. Oecologia 95: 565-574.

718 Dawson, T.E. 1996. Determining water use by trees and forests from isotopic, energy balance
719 and transpiration analyses: the roles of tree size and hydraulic lift. Tree Physiology 16:
720 263-272. doi:10.1093/treephys/16.1-2.263.
721 Dawson, T.E., S. Mambelli, A.H. Plamboeck, P.H. Templer and K.P. Tu. 2002. Stable isotopes
722 in plant ecology. Annual Review of Ecology and Systematics 33: 507-559.
723 de Groot, P.A. 2009. Handbook of stable isotope analytical techniquesElsevier, New York.
724 De Laeter, J.R., J.K. Böhlke, P. De Bièvre, H. Hidaka, H.S. Peiser, K.J.R. Rosman, et al. 2003.
725 Atomic weights of the elements: Review 2000. Pure and Applied Chemistry 75: 683-800.
726 Ehleringer, J. and T.E. Dawson. 1992. Water uptake by plants: perspectives from stable isotope
727 composition. Plant Cell and Environment 15: 1073-1082.
728 Ehleringer, J.R., S. Schwinning and R. Gebauer. 1999. Water use in arid land ecosystems. In: M.
729 C. Press, editor Advances in Plant Physiological Ecology. Blackwell Science, Oxford. p.
730 347-365.
731 Ellsworth, P.Z. and D.G. Williams. 2007. Hydrogen isotope fractionation during water uptake by
732 woody xerophytes. Plant and Soil 291: 93-107. doi:10.1007/s11104-006-9177-1.
733 Feddes, R.A., H. Hoff, M. Bruen, T. Dawson, P. de Rosnay, P. Dirmeyer, et al. 2001. Modeling
734 root water uptake in hydrological and climate models. Bulletin of the American
735 Meteorological Society 82: 2797-2809.
736 Flanagan, L.B. and J.R. Ehleringer. 1991. Stable isotope composition of stem and leaf water:
737 applications to the study of plant water use. Functional Ecology 5: 270-277.
738 Gat, J.R. 1996. Oxygen and hydrogen isotopes in the hydrologic cycle. Annual Review of Earth
739 and Planetary Sciences 24: 225-262.

740 Gee, G.W., M.D. Campbell, G.S. Campbell and J.H. Campbell. 1992. Rapid mearurement of low
741 soil-water potential using a water activity meter. Soil Science Society of America Journal
742 56: 1068-1070.
743 Gonfiantini, R. 1978. Standards for stable isotope measurments in natural compounds. Nature
744 271: 534-536. doi:10.1038/271534a0.
745 Griffis, T., J. Baker, S. Sargent, B. Tanner and J. Zhang. 2004. Measuring field-scale isotopic
746 CO_2 fluxes with tunable diode laser absorption spectroscopy and micrometeorological
747 techniques. Agricultural and Forest Meteorology 124: 15-29.
748 Griffis, T.J., S.D. Sargent, X. Lee, J.M. Baker, J. Greene, M. Erickson, et al. 2010. Determining
749 the oxygen isotope composition of evapotranspiration using eddy covariance. Boundary-
750 Layer Meteorology 137: 307-326.
751 Han, L.-F., M. Groening, P. Aggarwal and B.R. Helliker. 2006. Reliable determination of
752 oxygen and hydrogen isotope ratios in atmospheric water vapour adsorbed on 3A
753 molecular sieve. Rapid Communications in Mass Spectrometry 20: 3612-3618.
754 doi:10.1002/rcm.2772.
755 Hanisco, T.F., E.J. Moyer, E.M. Weinstock, J.M. St. Clair, D.S. Sayres, J.B. Smith, et al. 2007.
756 Observations of deep convective influence on stratospheric water vapor and its isotopic
757 composition. Geophysical Research Letters 34: L04814. doi:10.1029/2006gl027899.
758 Harmathy, T.Z. 1969. Simultaneous moisture and heat transfer in porous systems with particular
759 reference to drying. National Research Council of Canada. Ottawa. Research Paper No.
760 407.

761 Haverd, V. and M. Cuntz. 2010. Soil–Litter–Iso: A one-dimensional model for coupled transport
762 of heat, water and stable isotopes in soil with a litter layer and root extraction. Journal of
763 Hydrology 388: 438-455.
764 Haverd, V., M. Cuntz, D. Griffith, C. Keitel, C. Tadros and J. Twining. 2011. Measured
765 deuterium in water vapour concentration does not improve the constraint on the
766 partitioning of evapotranspiration in a tall forest canopy, as estimated using a soil
767 vegetation atmosphere transfer model. Agricultural and Forest Meteorology 151: 645-
768 654. doi:10.1016/j.agrformet.2011.02.005.
769 Helliker, B.R. and S.L. Richter. 2008. Subtropical to boreal convergence of tree-leaf
770 temperatures. Nature 454: 511-514.
771 Helliker, B.R., J.S. Roden, C. Cook and J.R. Ehleringer. 2002. A rapid and precise method for
772 sampling and determining the oxygen isotope ratio of atmospheric water vapor. Rapid
773 Communications in Mass Spectrometry 16: 929-932. doi:10.1002/rcm.659.
774 Henschel, J.R. and M.K. Seely. 2008. Ecophysiology of atmospheric moisture in the Namib
775 Desert. Atmospheric Research 87: 362-368.
776 Herbstritt, B., B. Gralher and M. Weiler. 2012. Continuous in situ measurements of stable
777 isotopes in liquid water. Water Resources Research 48: W03601.
778 Hesterberg, R. and U. Siegenthaler. 1991. Production and stable isotopic composition of CO2 in
779 a soil near Bern, Switzerland. Tellus 43B: 197-205.
780 Hoffmann, G., J. Jouzel and V. Masson. 2000. Stable water isotopes in atmospheric general
781 circulation models. Hydrological Processes 14: 1385-1406.

Horita, J. 2005. Saline waters. In: P. K. Aggarwal, J. R. Gat and K. F. O. Froehlich, editors, Isotopes in the water cycle: Past, present and future of a developing science. IAEA, Netherlands. p. 271-287.

Horita, J., K. Rozanski and S. Cohen. 2008. Isotope effects in the evaporation of water: a status report of the Craig-Gordon model. Isotopes in Environmental and Health Studies 44: 23-49. doi:10.1080/10256010801887174.

Horita, J. and D.J. Wesolowski. 1994. Liquid-vapor fractionation of oxygen and hydrogen isotopes of water from the freezing to the critical temperature. Geochimica et Cosmochimica Acta 58: 3425-3437. doi:10.1016/0016-7037(94)90096-5.

Hsieh, J.C.C., S.M. Savin, E.F. Kelly and O.A. Chadwick. 1998. Measurement of soil-water $\delta^{18}O$ values by direct equilibration with CO_2. Geoderma 82: 255-268.

2010. Measurements of CO2 carbon stable isotopes at artificial and natural analog sites. AGU Fall Meeting, San Francisco.

Jackson, R., L. Moore, W. Hoffman, W. Pockman and C. Linder. 1999. Ecosystem rooting depth determined with caves and DNA. Proceedings of the National Academy of Sciences 96: 11387-11392.

Jacob, H. and C. Sonntag. 1991. An 8-year record of the seasonal variation of H-2 and O-18 in atmospheric water vapor and precipitation at Heidelberg, Germany. Tellus Series B-Chemical and Physical Meteorology 43: 291-300. doi:10.1034/j.1600-0889.1991.t01-2-00003.x.

Japas, M.L., R. Fernandez-Prini, J. Horita and D.J. Wesolowski. 1995. Fractioning of isotopic species between coexisting liquid and vapor water: Complete temperature range,

804 including the asymptotic critical behavior. Journal of Physical Chemistry 99: 5171-5175.
805 doi:10.1021/j100014a043.
806 Jouzel, J. and R.D. Koster. 1996. A reconsideration of the initial conditions used for stable water
807 isotope models. Journal of Geophysical Research-Atmospheres 101: 22933-22938.
808 doi:10.1029/96jd02362.
809 Keeling, C.D. 1958. The concentration and isotopic abundances of atmospheric carbon dioxide
810 in rural areas. Geochimica et Cosmochimica Acta 13: 322-324.
811 Kelly, S.F. and J.S. Selker. 2001. Osmotically driven water vapor transport in unsaturated soils.
812 Soil Science Society of America Journal 65: 1634-1641.
813 Kerstel, E.R.T., R. van Trigt, N. Dam, J. Reuss and H.A.J. Meijer. 1999. Simultaneous
814 determination of the H-2/H-1, O-17/O-16, and O-18/O-16 isotope abundance ratios in
815 water by means of laser spectrometry. Analytical Chemistry 71: 5297-5303.
816 doi:10.1021/ac990621e.
817 Kim, K. and X. Lee. 2011. Isotopic enrichment of liquid water during evaporation from water
818 surfaces. Journal of Hydrology 399: 364-375. doi:10.1016/j.jhydrol.2011.01.008.
819 Lee, J.-E., I. Fung, D.J. DePaolo and C.C. Henning. 2007. Analysis of the global distribution of
820 water isotopes using the NCAR atmospheric general circulation model. Journal of
821 Geophysical Research 112: D16306.
822 Lee, X. and W. Massman. 2011. A perspective on thirty years of the Webb, Pearman and
823 Leuning density corrections. Boundary-Layer Meteorology 139: 39-59.
824 Lee, X., S. Sargent, R. Smith and B. Tanner. 2005. In situ measurements of the water vapor
825 $^{18}O/^{16}O$ isotope ratio for atmospheric and ecological applications. Journal of Atmospheric
826 and Oceanic Technology 22: 555-565.

827 Luz, B., E. Barkan, R. Yam and A. Shemesh. 2009. Fractionation of oxygen and hydrogen
828 isotopes in evaporating water. Geochimica et Cosmochimica Acta 73: 6697-6703.
829 doi:10.1016/j.gca.2009.08.008.
830 Majoube, M. 1971. Oxygen-18 and deuterium fractionation between water and steam. Journal De
831 Chimie Physique Et De Physico-Chimie Biologique 68: 1423-1438.
832 Mathieu, R. and T. Bariac. 1996. A numerical model for the simulation of stable isotope profiles
833 in drying soils. Journal of Geophysical Research 101: 685-696.
834 Melayah, A., L. Bruckler and T. Bariac. 1996a. Modeling the transport of water stable isotopes
835 in unsaturated sails under natural conditions .1. Theory. Water Resources Research 32:
836 2047-2054. doi:10.1029/96wr00674.
837 Melayah, A., L. Bruckler and T. Bariac. 1996b. Modeling the transport of water stable isotopes
838 in unsaturated soils under natural conditions .2. Comparison with field experiments.
839 Water Resources Research 32: 2055-2065. doi:10.1029/96wr00673.
840 Merlivat, L. 1978. Molecular diffusivities of $H_2{}^{16}O$, $HD^{16}O$, and H_2O-^{18}O in gases. Journal of
841 Chemical Physics 69: 2864-2871. doi:10.1063/1.436884.
842 Midwood, A.J., B. Thornton and P. Millard. 2008. Measuring the (13)C content of soil-respired
843 CO(2) using a novel open chamber system. Rapid Communications in Mass
844 Spectrometry 22: 2073-2081. doi:10.1002/rcm.3588.
845 Mooney, H.A., S.L. Gulmon, P.W. Rundel and J. Ehleringer. 1980. Further Observations on the
846 Water Relations of Prosopis-Tamarugo of the Northern Atacama Desert. Oecologia 44:
847 177-180.
848 Nicholson, S. 2000. Land surface processes and sahel climate. Reviews of Geophysics 38: 117-
849 139.

850 Ogée, J., P. Peylin, M. Cuntz, T. Bariac, Y. Brunet, P. Berbigier, et al. 2004. Partitioning net
851 ecosystem carbon exchange into net assimilation and respiration with canopy-scale
852 isotopic measurements: An error propagation analysis with $^{13}CO_2$ and $CO^{18}O$ data.
853 Global Biogeochemical Cycles 18: GB2019. doi:10.1029/2003gb002166.
854 Oi, T. 2003. Vapor pressure isotope effects of water studied by molecular orbital calculations.
855 Journal of Nuclear Science and Technology 40: 517-523. doi:10.3327/jnst.40.517.
856 Panday, S. and P.S. Huyakorn. 2008. MODFLOW SURFACT: A state-of-the-art use of vadose
857 zone flow and transport equations and numerical techniques for environmental
858 evaluations. Vadose Zone Journal 7: 610-631.
859 Peters, L.I. and D. Yakir. 2010. A rapid method for the sampling of atmospheric water vapour
860 for isotopic analysis. Rapid Communications in Mass Spectrometry 24: 103-108.
861 doi:10.1002/rcm.4359.
862 Philip, J.R. and D.A. de Vries. 1957. Moisture movement in porous materials under temperature
863 gradients. Transactions of the American Geophysical Union 38: 222–232.
864 Phillips, F.M. and H.W. Bentley. 1987. Isotopic fractionation during ion filtration: 1. Theory.
865 Geochimica et Cosmochimica Acta 51: 683-695.
866 Pollack, W., L.E. Heidt, R. Lueb and D.H. Ehhalt. 1980. Measurement of stratospheric water
867 vapour by cryogenic collection. Journal of Geophysical Research 85: 5555-5568.
868 Polyakov, V.B., J. Horita, D.R. Cole and A.A. Chialvo. 2007. Novel corresponding-states
869 principle approach for the equation of state of isotopologues: (H2O)-O-18 as an example.
870 Journal of Physical Chemistry B 111: 393-401. doi:10.1021/jp064055k.

871 Richard, T., L. Mercury, M. Massault and J.L. Michelot. 2007. Experimental study of D/H
872 isotopic fractionation factor of water adsorbed on porous silica tubes. Geochimica et
873 Cosmochimica Acta 71: 1159-1169.
874 Risi, C., S. Bony, F. Vimeux, C. Frankenberg, D. Noone and J. Worden. 2010a. Understanding
875 the Sahelian water budget through the isotopic composition of water vapor and
876 precipitation. Journal of Geophysical Research-Atmospheres 115: D24110.
877 doi:10.1029/2010jd014690.
878 Risi, C., S. Bony, F. Vimeux and J. Jouzel. 2010b. Water-stable isotopes in the LMDZ4 general
879 circulation model: Model evaluation for present-day and past climates and applications to
880 climatic interpretations of tropical isotopic records. Journal of Geophysical Research-
881 Atmospheres 115: D24123. doi:10.1029/2010jd015242.
882 Rodriguez-Iturbe, I. and A. Porporato. 2004. Ecohydrology of water-controlled ecosystems: Soil
883 moisture and plant dynamicsCambridge University Press, Cambridge.
884 Rothfuss, Y., P. Biron, I. Braud, L. Canale, J.-L. Durand, J.-P. Gaudet, et al. 2010. Partitioning
885 evapotranspiration fluxes into soil evaporation and plant transpiration using water stable
886 isotopes under controlled conditions. Hydrological Processes 24: 3177-3194.
887 doi:10.1002/hyp.7743.
888 Rozanski, K. 2005. Isotopes in atmospheric moisture. In: P. K. Aggarwal, J. R. Gat and K. F. O.
889 Froehlich, editors, Isotopes in the water cycle: Past, present and future of a developing
890 science. IAEA, Netherlands. p. 291-302.
891 Scanlon, T.M., K.K. Caylor, S. Levin and I. Rodriguez-Iturbe. 2007. Positive feedbacks promote
892 power-law clustering of Kalahari vegetation. Nature 449: 209-213.

Schneider, M., K. Yoshimura, F. Hase and T. Blumenstock. 2010. The ground-based FTIR network's potential for investigating the atmospheric water cycle. Atmospheric Chemistry and Physics 10: 3427-3442.

Scrimgeour, C.M. 1995. Measurement of plant and soil water isotope composition by direct equilibration methods. Journal of Hydrology 173: 261-274.

Shurbaji, A.R.M. and F.M. Phillips. 1995. A numerical-model for the movement of H_2O, $H_2{}^{18}O$, and ^2HHO in the unsaturated zone. Journal of Hydrology 171: 125-142.

Sofer, Z. and J.R. Gat. 1975. Isotope composition of evaporating brines - effect of isotopic activity ratio in saline solutions. Earth and Planetary Science Letters 26: 179-186.

Stewart, G.L. 1972. Clay-water interaction, behavior of ^3H and ^2H in adsorbed water, and isotope effect. Soil Science Society of America Proceedings 36: 421-426.

Striegl, R.G. 1988. Distribution of gases in the unsaturated zone at a low-level radioactive-waste disposal site near Sheffield, Illinois. U.S. Geological Survey. Urbana, Illinois. Water-Resources Investigations Report 88-4025.

Syvertsen, J.P., G.L. Cunningham and T.V. Feather. 1975. Anomalous diurnal patterns of stem xylem water potentials in *Larrea tridentata*. Ecology 56: 1423-1428.

Tang, K.L. and X.H. Feng. 2001. The effect of soil hydrology on the oxygen and hydrogen isotopic compositions of plants' source water. Earth and Planetary Science Letters 185: 355-367.

Twining, J., D. Stone, C. Tadros, A. Henderson-Sellers and A. Williams. 2006. Moisture Isotopes in the Biosphere and Atmosphere (MIBA) in Australia: A priori estimates and preliminary observations of stable water isotopes in soil, plant and vapour for the Tumbarumba Field Campaign. Global and Planetary Change 51: 59-72.

916 Walker, G.R., P.H. Woods and G.B. Allison. 1994. Interlaboratory comparison of methods to
917 determine the stable isotope composition of soil water. Chemical Geology 111: 297-306.
918 Wang, L., K. Caylor and D. Dragoni. 2009. On the calibration of continuous, high-precision $\delta^{18}O$
919 and $\delta^{2}H$ measurements using an off-axis integrated cavity output spectrometer. Rapid
920 Communications in Mass Spectrometry 23: 530-536.
921 Wang, L., K.K. Caylor, J. Camilo Villegas, G.A. Barron-Gafford, D.D. Breshears and T.E.
922 Huxman. 2010. Partitioning evapotranspiration across gradients of woody plant cover:
923 assessment of a stable isotope technique. Geophysical Research Letters 37: L09401.
924 doi:10.1029/2010GL043228.
925 Wang, L., S. Good, K. Caylor and L.A. Cernusak. 2012. Direct quantification of leaf
926 transpiration isotopic composition. Agricultural and Forest Meteorology 154-155: 127-
927 135.
928 Warren, J., J. Brooks, M. Dragila and F. Meinzer. 2011. In situ separation of root hydraulic
929 redistribution of soil water from liquid and vapor transport. Oecologia 166: 899-911.
930 Wassenaar, L.I., M.J. Hendry, V.L. Chostner and G.P. Lis. 2008. High resolution pore water $\delta^{2}H$
931 and $\delta^{18}O$ measurements by $H_2O_{(liquid)}$-$H_2O_{(vapor)}$ equilibration laser spectroscopy.
932 Environmental Science & Technology 42: 9262-9267. doi:10.1021/es802065s.
933 Webster, C.R. and A.J. Heymsfield. 2003. Water isotope ratios D/H, $^{18}O/^{16}O$, $^{17}O/^{16}O$ in and out
934 of clouds map dehydration pathways. Science 302: 1742-1745.
935 Welp, L.R., R.F. Keeling, H.A.J. Meijer, A.F. Bollenbacher, S.C. Piper, K. Yoshimura, et al.
936 2011. Interannual variability in the oxygen isotopes of atmospheric CO2 driven by El
937 Nino. Nature 477: 579-582.

West, A.G., S.J. Partrickson and J.R. Ehleringer. 2006. Water extraction times for plant and soil materials used in stable isotope analysis. Rapid Communications in Mass Spectrometry 20: 1317-1321.

White, J.W.C., E.R. Cook, J.R. Lawrence and W.S. Broecker. 1985. The D/H ratios of sap in trees: Implications for water sources and tree ring D/H ratios. Geochimica Et Cosmochimica Acta 49: 237-246.

Wingate, L., J. Ogée, M. Cuntz, B. Genty, I. Reiter, U. Seibt, et al. 2009. The impact of soil microorganisms on the global budget of $d^{18}O$ in atmospheric CO_2. Proceedings of the National Academy of Sciences 106: 22411-22415.

Wingate, L., U. Seibt, K. Maseyk, J. Ogée, P. Almeida, D. Yakir, et al. 2008. Evaporation and carbonic anhydrase activity recorded in oxygen isotope signatures of net CO_2 fluxes from a Mediterranean soil. Global Change Biology 14: 2178-2193.

Worden, J., D. Noone, K. Bowman and T.E. Spect. 2007. Importance of rain evaporation and continental convection in the tropical water cycle. Nature 445: 528-532. doi:Doi 10.1038/Nature05508.

Yakir, D. and L.D.L. Sternberg. 2000. The use of stable isotopes to study ecosystem gas exchange. Oecologia 123: 297-311.

Yakir, D. and X.-F. Wang. 1996. Fluxes of CO_2 and water between terrestrial vegetation and the atmosphere estimated from isotope measurements. Nature 380: 515-517.

Yamanaka, T. and R. Shimizu. 2007. Spatial distribution of deuterium in atmospheric water vapor: Diagnosing sources and the mixing of atmospheric moisture. Geochimica et Cosmochimica Acta 71: 3162-3169.

960 Yepez, E., D. Williams, R. Scott and G. Lin. 2003. Partitioning overstory and understory
961 evapotranspiration in a semiarid savanna woodland from the isotopic composition of
962 water vapor. Agricultural and Forest Meteorology 119: 53-68.
963 Yoshimura, K., S. Miyazaki, S. Kanae and T. Oki. 2006. Iso-MATSIRO, a land surface model
964 that incorporates stable water isotopes. Global and Planetary Change 51: 90-107.
965 doi:10.1016/j.gloplacha.2005.12.007.
966 Yu, W., T. Yao, L. Tian, Y. Wang and C. Yin. 2005. Isotopic composition of atmospheric water
967 vapor before and after the monsoon's end in the Nagqu River Basin. Chinese Science
968 Bulletin 50: 2755-2760.
969 Zimmerman, U., D. Ehhalt and K.O. Munnich. 1967. Soil-water movement and
970 evapotranspiration: Changes in the isotopic composition of the water. In: IAEA, editor
971 Isotopes in hydrology; Proceedings of the symposium (1966: Vienna). International
972 Atomic Energy Agency, Vienna. p. 567-585.

973

974

975 Table 1: Summary of measurement and modeling techniques to quantify isotopic compositions
976 of soil water vapor and soil evaporation.

Potential methods	Notes	References
Measurement:		
Isothermal equilibrium (H_2O, CO_2, H_2)†	Inside the laboratory	Stewart 1972, Scrimgeour 1995, Hsieh et al. 1998, Richard et al. 2007, Wassenaar et al. 2008
In situ CO_2-H_2O equilibrium†	In vadose zone	Hesterberg and Siegenthaler 1991, Hsieh et al. 1998, Tang and Feng 2001, Wingate et al. 2008
Cryogenic soil column vapor collection	Inside the laboratory	Zimmerman 1967, Stewart 1972, Braud et al. 2009ab; Rothfuss et al. 2010
In situ cryogenic soil gas sampling	In vadose zone	Striegl 1988, references in Mathieu and Bariac 1996
In situ sealed chamber	From soil surface	Haverd et al. 2011
Open chamber with mass balance	From soil surface	Wang et al. 2012
In situ direct measurement with laser spectroscopy	In vadose zone	This manuscript
Modeling:		
Craig-Gordon Model	Formulated for free water evaporation	Craig and Gordon 1965, Horita et al. 2008
Analytical isotope transport models		Zimmerman et al. 1967, Barnes and Allison 1983
Numerical isotope transport models	Varied results, but capture the shape of observations well	Shurbaji and Phillips 1995, Mathieu and Bariac 1996, Melayah et al. 1996a,b, Braud et al. 2005a,b, Braud et al. 2009ab, Harverd and Cuntz 2010, Haverd et al. 2011

977 † - These methods are used to estimate liquid soil water isotopic composition, but the details of
978 the equilibrium and sampling methods are relevant to soil water vapor isotopes.

Table 2: Liquid-vapor isotopic fractionation factors for water. See Horita et al. (2008) for compiled historical values. Equilibrium values are listed for 25 °C unless noted.

	$\alpha_{L/V}(^{18}O)$	$\alpha_{L/V}(^{2}H)$	**Description**	**Ref.**
Equilibrium:				
Best current values (empirical)	1.00935	1.07875	Combination of evaporation experiments	1
ab initio	*1.008†*	*1.107*	*HF calculation level*	2
ab initio	*1.013*	*1.145*	*B3LYP calculation level*	2
Molecular simulation	*1.016*	*1.622*	*Gaussian charge polarizable*	3
Molecular simulation	*1.018*	*1.612*	*Nonpolarizable extended simple point charge*	3
Thermodynamics	*1.0094*	*1.0798*	*Corresponding states principle*	4,5
Empirical - dried clay	NA	1.04‡	See text	6
Empirical - silica tubes	NA	1.055§	See text	7
Kinetic (*D*/*Di*):				
Best current values (empirical)	1.0285	1.0251	Evaporation at 20 ºC in air	8
	1.0281	1.0249	Evaporation at 20 ºC in N2	8
Recent experiment	1.0275	1.0230	Values from the 20.1 ºC experiment in air	9
Gas kinetic theory	*1.0323*	*1.0166*	*In dry air; Isotopologues have identical collision diameters*	10
Gas kinetic theory	*1.0319*	*1.0164*	*In N_2; Isotopologues have identical collision diameters*	11

Italics indicate modeled values.

References: 1 - Horita and Wesolowski 1994; 2 - Oi 2003; 3 - Chialvo and Horita 2009; 4 - Japas et al. 1995; 5 - Polyakov et al. 2007; 6 - Stewart 1972; 7 - Richard et al. 2007; 8 - Merlivat 1978; 9 - Luz et al. 2009; 10 - Horita et al. 2008; 11 - Cappa et al. 2003

† – All equilibrium model values (*ab initio*, molecular dynamic, and thermodynamic) are estimated from Figures 4, 6 and 8 from Chialvo and Horita (2009); *ab initio* means "from first principles"

‡ - Temperature unknown -- listed as "room temperature"; the listed $\alpha_{L/V}(^{2}H)$ value (1.04) is the median of 0.93 to 1.06 (n = 7), see text for details.

§ - Temperature is 20 ºC rather than 25 ºC. The free water $\alpha_{L/V}(^2H)$ value at 20 ºC is 1.08453 from Equation 3. The listed value (1.055) was the maximum observed, corresponding to relative humidity (RH) values above ~70%. Lower RH conditions corresponded to lower values of $\alpha_{L/V}(^2H)$ down to around 1.30 at 10% RH.

996 Table 3: Craig-Gordon model parameters, and example calculations of δ_E for free water and soil
997 water. The example data were collected on 29 March 2011 at Mpala Research Center, Kenya,
998 from a soil profile fitted with buried Teflon tubing from which air was drawn directly into a
999 Water Vapor Isotope Analyzer (DLT-100, Los Gatos Research Inc., Mountain View, CA).

Parameter	**Example – Mean of 5, 10, 20, and 30 cm**		**Example – 5 cm**		**Typical range**	
T_A	302		302		280 to 310	
T_0	300		301		290 to 320	
h_A	0.331		0.331		0.2 to 0.6	
$h_A'(T)$	0.374		0.351		0.2 to 1.0	
$h_A'(T, \psi)$	0.429		0.433			
ψ_0	**-18.8**		**-29.2**		-1 to -100	
θ_0	0.0602		0.0525		0.01 to 0.45	
θ_s	0.45		0.45		0.2 to 0.5	
θ_r	0.035		0.035		0.01 to 0.05	
Depth min [cm]	5		5		10 to 50‡	
Depth max [cm]	30		5			
n (θ)	0.970		0.979		0.5 to 1.0	
n (free water)	0.5		0.5		0.5	
	$\delta^{18}O$	**$\delta^{2}H$**	**$\delta^{18}O$**	**$\delta^{2}H$**	**$\delta^{18}O$**	**$\delta^{2}H$**
$\alpha_{e,L/V}$	1.009206	1.07693	1.009117	1.07579	1.008 to 1.010	1.059 to 1.088
D/D_i	1.0285	1.0251	1.0285	1.0251	1.028 to 1.032	1.016 to 1.025
$\varepsilon_{k,L/V}(\theta,T)$	0.01728	0.01523	0.01810	0.01596	0.001 to 0.023	0.001 to 0.020
$\varepsilon_{k,L/V}(\theta,T,\psi)$	0.01578	0.01391	0.01581	0.01394		
$\varepsilon_{k,L/V}$(free water,T)	0.00891	0.00786	0.00925	0.00815	0.001 to 0.014	0.001 to 0.013
r_m/r	1	1	1	1	0.5 to 1.0	0.5 to 1.0
δ_L	**6.2**†	**6.5**	**13.2**	**26.2**	-5 to 10	-30 to 30
δ_V (meas)	-2.8	-56.6	-2.2	-54.6	NA	NA
δ_V (equil)	-3.0	-65.4	4.1	-46.1	-15 to 3.0	-120 to -30
δ_A	-10.4	-68.7	-10.4	-68.7	-10 to -20	-50 to -150
Calculated Evaporate:						
δ_E (θ,T)	-25.6	-94.3	-15.7	-65.1		
δ_E (θ,T,ψ)	-24.5	-94.6	-12.6	-61.3		
δ_E (free water,T)	-12.7	-83.7	-2.5	-54.0		

1000 ‡ Typical evaporating front depth from Barnes and Allison (1988)

† - All isotope values are presented here in per mil notation (δ x 1000), whereas in calculations they are converted to decimal notation (e.g. Equation 4, resulting in -25.6 ‰ for "$\delta_E(\theta, T)$" in column 2 above):

$$\delta_E = \frac{\left(0.0062/1.009206\right) - 0.374(-0.0104) - 0.009206 - 0.01728}{1 - 0.374 + 0.01728} = -0.0256$$

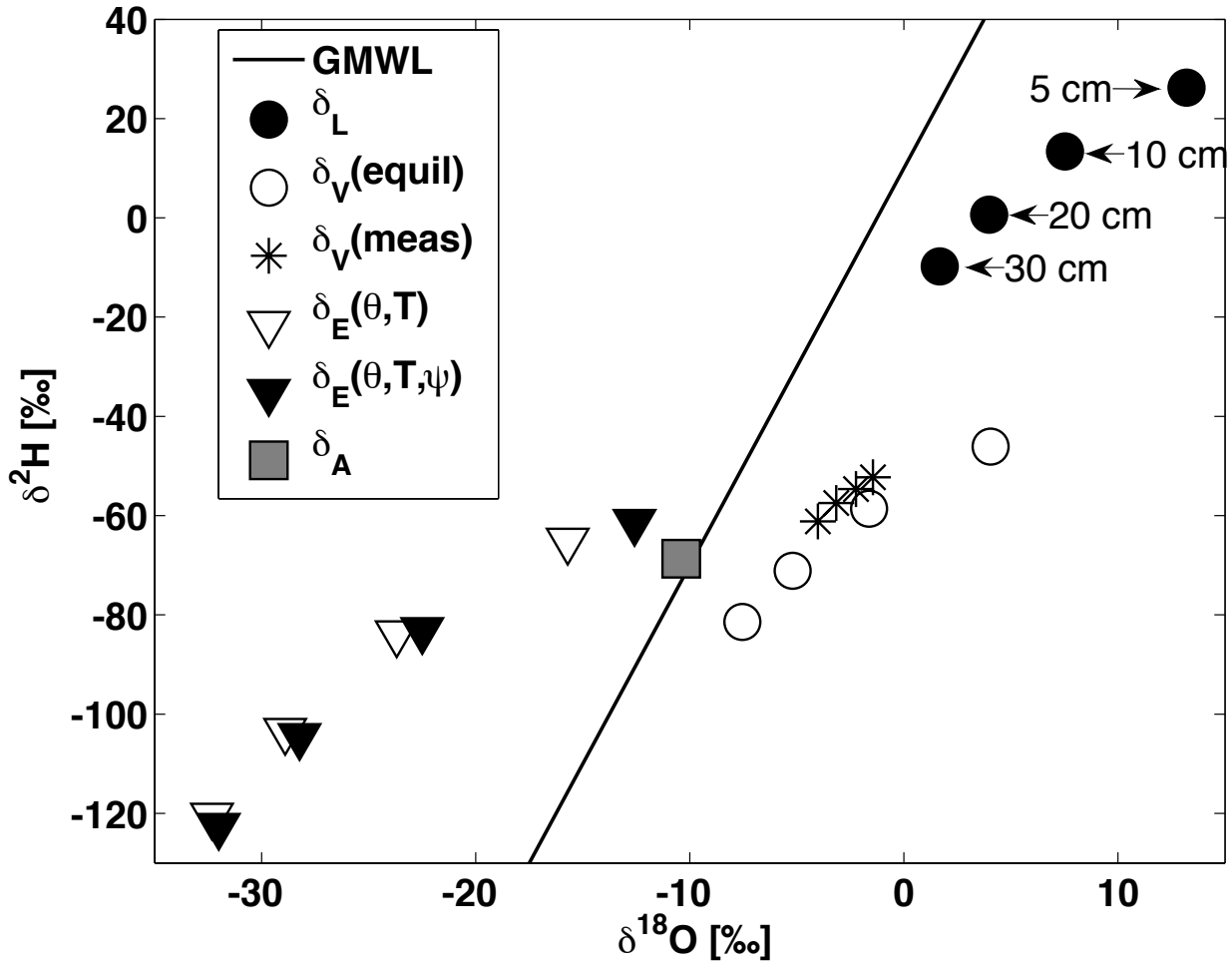

1006

1007 Figure 1: Measured and calculated isotope values of liquid and vapor phase water from a soil
1008 profile sampled 29 March 2011 in sandy loam soil at Mpala Research Center, Kenya (see Section
1009 4 and Table 3). Sampling depths are shown for the liquid soil water samples, and each set of
1010 vapor values follows the same depth sequence. Two sets of δ_V values are shown: "$\delta_{V(meas)}$" was
1011 measured directly in the field with a Water Vapor Isotope Analyzer (DLT-100, Los Gatos
1012 Research Inc., Mountain View, CA); "$\delta_{V(equil)}$" was calculated using soil temperature and liquid
1013 soil water isotopic composition (Equations 1 to 3). Craig-Gordon model δ_E values were
1014 calculated in two ways: "$\delta_{E(\theta,T)}$" was calculated conventionally, considering volumetric water

content and soil temperature (Equations 2 to 8); "$\delta_E(\theta,T,\psi)$" was calculated by additionally considering soil water potential (Equations 2 to 9).

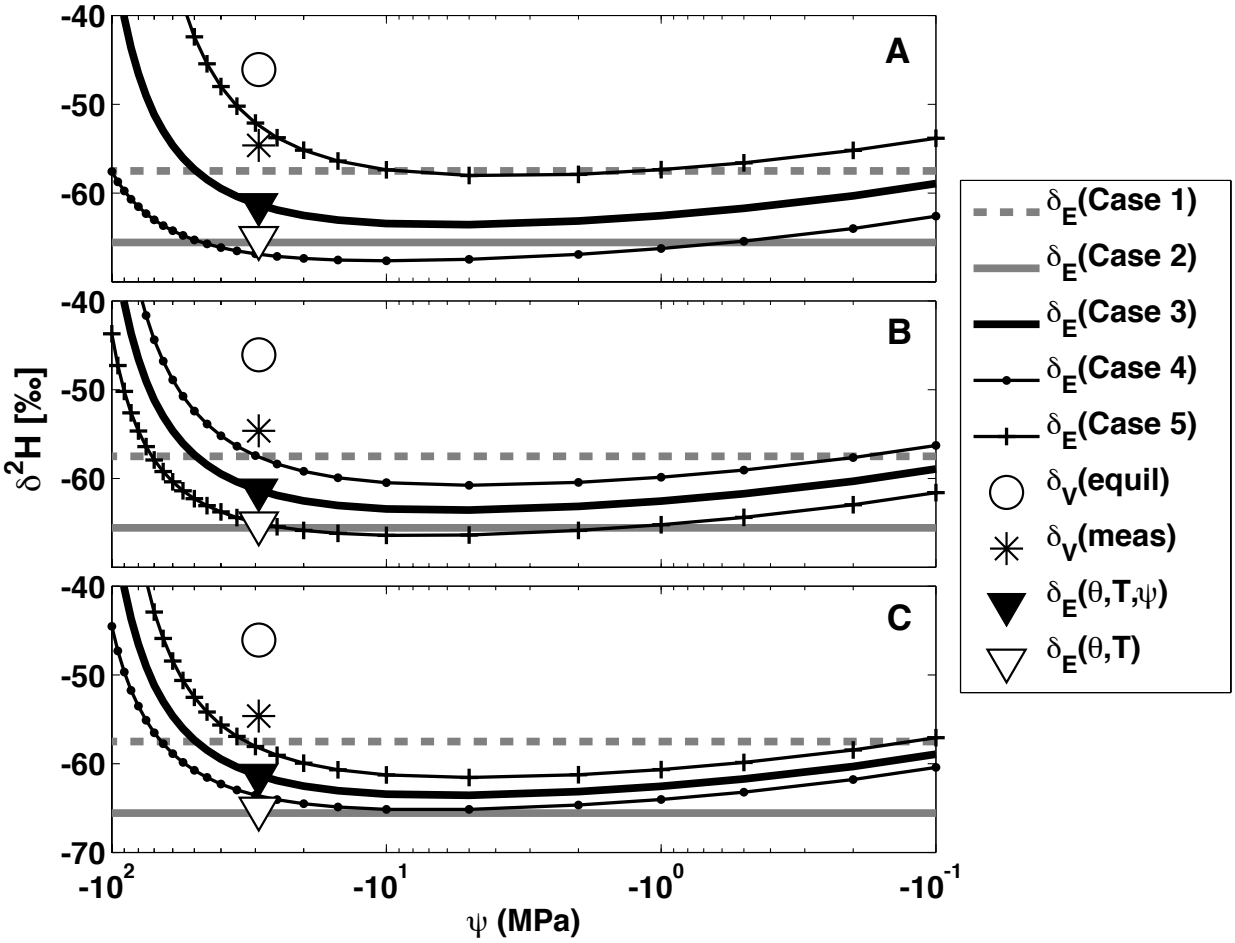

Figure 2: Craig-Gordon model calculations (Equations 2 to 9) for δ^2H across a range of soil water potentials (ψ) and ambient atmospheric parameters. The measured and calculated parameters for the 5 cm depth example of Table 3 and Figure 1 are used as a starting point, and these values are shown with the same symbols as in Figure 1. Each panel shows five "Cases." Cases 1 and 2 were calculated without considering soil moisture content or soil water potential (i.e., $n = 1$ and $a_w = 1$), and use the contrasting α_k values of Cappa et al. (2003) and Merlivat (1978), respectively. Cases 3, 4 and 5 show the effects of varying one of three atmospheric parameters: relative humidity (h_A) in panel A, water vapor isotopic composition (δ_A) in panel B, and temperature (T_A) in panel C. Case 3 always uses the measured values ($h_A = 0.331$, $\delta_A = -68.7$

1027 ‰, T_A = 28.8 °C), whereas Cases 4 and 5 use lower and higher bounds, respectively, of a range

1028 that one could expect in the field (h_A ± 0.1, δ_A ± 5 ‰, and T_A ± 2 °C).

1029
1030